PHYSICAL REVIEW B VOLUME 35, NUMBER 16 1 JUNE 1987

Theory of ultrasonic attenuation in impure anisotropic *p*-wave superconductors

L. Coffey*
Theoretische Physik, Eidgenössische Technische Hochschule Honggerberg, Zurich, 8093, Switzerland
(Received 22 September 1986; revised manuscript received 1 December 1986)

The longitudinal ultrasonic attenuation for impure anisotropic superconductors in the axial and polar phases is calculated using the deformation-potential approach. Impurity effects are treated by the self-consistent Born method. For realistic values of ql and $\omega\tau$, good agreement is obtained between theory and experiments. This is the case for the exponents describing the intermediate temperature dependence as well as the peak observed in the sound attenuation just below T_c. The behavior of the peak that is calculated in this theory is examined and discussed.

INTRODUCTION

Recent experiments[1–4] on longitudinal ultrasonic attenuation $[\alpha(T)]$ in the heavy-fermion superconductors UPt_3 and UBe_{13} have yielded results that differ markedly from the predictions of BCS theory. The low-temperature (T) behavior of $\alpha(T)$ has either a T^2 (Refs. 1 and 2) or a T^3 (Ref. 3) dependence rather than the exponential behavior of BCS theory. These results are interpreted as evidence for an anisotropic order parameter in these materials. Furthermore, the experiments[1–4] have observed a pronounced peak in $\alpha(T)$ just below the superconducting transition temperature T_c. The experiments are all carried out in the hydrodynamic regime judging by the ω^2 dependence of many of the experimental features. Here ω is the sound-wave frequency.

Several theoretical studies,[5–10] some using group theoretical techniques, have led to conclusions concerning the nature of the anisotropic superconducting order parameter in these materials. One conclusion of these studies is that while *p*-wave superconducting states can have order parameters with point zeros on the Fermi surface (axial), order parameters with line zeros (polar) appear to be ruled out when considerations of crystal symmetry are taken into account. The hope has been to use studies of transport properties, in particular ultrasonic attenuation, to lend support to these conclusions. Another goal is to get a more accurate picture of the anisotropy of the order parameter beyond the simple generic polar and axial type phases.

The first theoretical analysis[1] of the $\alpha(T)$ data for UPt_3 fitted the observed low-temperature T^2 dependence by means of a polar state. The same data was later reinterpreted[11] using a Boltzmann-equation approach in terms of an axial state. A further complication was introduced when a simple Born-approximation study of impurity scattering concluded[12] that the quasiparticle mean free paths (l) appear to diverge at low energies in both the axial and polar phases. When this effect is included in the Boltzmann equation approach, a nonzero sound attenuation at zero temperature $[\alpha(0)]$ is obtained in the superconducting state, equal to the normal-state sound attenuation (α_n).

A way to prevent this low-energy divergence of the mean free path and to support the conclusions of Ref. 11 is by means of resonant impurity scattering.[13] This approach builds in the effect of multiple scattering and makes use of the important assumption that the normal-state phase shift due to impurity scattering δ_n, is close to $\pi/2$. The same approach to impurity effects has been implemented self-consistently[14] in a general survey of thermal and transport properties. The conclusion of that work[14] is that the superconducting phase that best explains the experimental results is a polar phase.

Subsequent studies of $\alpha(T)$ in the axial and polar phases, using the resonant impurity scattering technique, have yielded mixed results. Without vertex corrections,[15] it was concluded that the experiments could be described best by a polar phase, although that work did not rule out the possibility of axial-type phases with certainty. However with the subsequent inclusion of vertex corrections,[16] it was concluded that an axial phase described the data best. Both of these calculations examined the $v_s/v_F=0$ limit, where v_s is the sound velocity and v_F is the quasiparticle Fermi velocity in the superconductor. The latter calculation plotted results for the $ql=0.0$ case only, where q is the sound wave vector. Neither of these studies observed a peak in $\alpha(T)$ below T_c.

However, an examination[17] of both phases in the clean limit detected a peak in $\alpha(T)$ whose shape and position depended on the choice of parameters in the theory. One parameter whose importance is pointed out in that work is the ratio of the superconducting critical temperature (T_c) to the Fermi temperature (T_F). For a heavy fermion material this parameter is chosen to be 0.1, among other values. The shapes of the curves obtained depend quite markedly on this ratio. However a related ratio, v_s/v_F, is still chosen to be zero, which is somewhat inconsistent.

It has also been proposed recently[18] that the experimentally observed peak in $\alpha(T)$ is due to a Landau-Khalatnikov relaxational mode of the order parameter. The scattering time associated with nonmagnetic impurity scattering (τ) plays a very important role in establishing this mechanism.

It has been experimentally observed[19] that the

Grüneisen parameter η has values ranging from 10 to 100 in heavy-fermion materials. The implications of this for sound attenuation in the normal state have been investigated recently.[20] This study concluded that the isothermal sound velocity is much smaller than the adiabatic sound velocity because of the large values for both η and the quasiparticle effective mass m_e^*. Furthermore, there will be a large contribution from heat conduction to $\alpha(T)$. The implications of this for sound attenuation in the superconducting state are unclear at the moment. The present study does not incorporate any such mechanism due to heat conduction in $\alpha(T)$ arising from the larger than usual value for η.

In the present work a careful numerical study of the longitudinal ultrasonic attenuation [$\alpha(T)$], using the conventional deformation potential approach, is carried out. Impurity scattering is treated within the standard self consistent Born approximation.[21,22] Thus the present calculation avoids any dependence on the normal-state phase shift δ_N, or the assumption that it should be close to $\pi/2$, as occurs in the resonant impurity scattering approach.[13] The self-consistent Born approximation was chosen since it is the conventional formalism within which to treat impurity scattering in these problems[21,22] and the final results of the present calculation for $\alpha(T)$ appear to justify this choice. The theory is set up for numerical computation in sufficiently general form to allow ql and $\omega\tau$ to be varied from values much larger to values much smaller than unity. Here q is the sound wave vector, l is the mean free path of quasiparticles due to nonmagnetic impurity scattering, ω is the sound wave frequency and τ is the scattering time due to impurities.

The calculation reproduces accurately the conventional BCS and normal state results for $\alpha(T)$ in the $ql \ll 1$ and $ql \gg 1$ limits. The theory is based essentially on the calculation of two dynamical electronic conductivities which arise in the formulation of the problem and which are in turn determined by the impurity averaged density-density correlation function.[21]

Very striking agreement is obtained between the theoretical results for $\alpha(T)$ in anisotropic superconducting states and the experimental observations. This is achieved in the hydrodynamical regime with realistic values for the parameters ql and $\omega\tau$. Not only are the observed low-temperature exponents in $\alpha(T)$ reproduced but so also is the peak in $\alpha(T)$ seen just below T_c.

Possible effects on $\alpha(T)$ due to inelastic electron-electron scattering processes are not included in the present calculation. These may be relevant in UBe_{13}. Furthermore the superconductivity is treated in the weak coupling approximation.

Apart from the Introduction, this paper is divided into two main sections. The first contains a general description of both the general theory for calculating $\alpha(T)$ and the treatment of impurity scattering. The second section presents and discusses the numerical results obtained from the present approach for both axial and polar phases. Suggestions for experimental tests of the predictions of the present calculation are also put forward in the second section. Finally a brief summary is provided in a concluding section.

GENERAL THEORY

This calculation, based on the conventional deformation potential idea, assumes that the ultrasonic attenuation is purely electronic in origin at the low temperatures under consideration.[21–23] The electrons in the material move in response to the time and spatially dependent electric field set up by the motion of the ionic lattice as the sound wave passes through. An energy balance is achieved in the electron gas in that the energy transferred to the electrons by this process is equal to the amount lost through Joule heating. Thus the ultrasonic attenuation coefficient is defined as

$$\alpha(T)=\tfrac{1}{2}\mathrm{Re}[\mathbf{j}_e^*\cdot\mathbf{E}]/\tfrac{1}{2}\rho\mathbf{u}^*\cdot\mathbf{u}c_s \ , \tag{1}$$

where $\mathbf{j}_e$ is the electronic current, $\mathbf{E}$ the macroscopic electric field in the solid, ρ the ionic density, $\mathbf{u}$ the ion velocity, and c_s the sound velocity.

The impurities move with the lattice and, in order to treat impurity scattering elastically, a unitary transformation is made to a rest frame moving with them.[21] In this rest frame the electrons respond to a perturbation due to the electromagnetic potential $\phi(q,\omega)$ [where $\mathbf{E}=-\nabla\phi(q,\omega)$] and to a new perturbation described by

$$H_I=\frac{1}{m_e^*\omega}\left[\mathbf{q}\cdot\left[\mathbf{p}+\frac{\mathbf{q}}{2}\right]\right]\left[\mathbf{u}\cdot\left[\mathbf{p}+\frac{\mathbf{q}}{2}\right]\right]-\mathbf{u}\cdot\left[\mathbf{p}+\frac{\mathbf{q}}{2}\right] , \tag{2}$$

where $\mathbf{q}$ is the sound-wave vector and $\mathbf{p}$ is the electron momentum vector. The electronic current is then given by

$$\mathbf{j}_e=\sigma(\mathbf{q},\omega)\mathbf{E}(q,\omega)-\frac{m_e^*\mathbf{u}}{e\tau}\sigma^I(\mathbf{q},\omega) \ . \tag{3}$$

In Eq. (3) $\sigma(\mathbf{q},\omega)$ and $\sigma^I(\mathbf{q},\omega)$ are the dynamical conductivities describing the response of the electron density (ρ_e) to $\phi(q,\omega)$ and H_I, respectively.

A self-consistent solution of $\mathbf{j}_e$ and $\mathbf{E}$ from both the Maxwell equations and the continuity equation for ρ_e yield[24]

$$\alpha(T)=\frac{nm_e^*}{\rho c_s\tau}\mathrm{Re}\left[\frac{\sigma_0-\sigma^I}{\sigma}\right] , \tag{4}$$

where $\sigma_0=ne^2\tau/m_e^*$. The explicit collision drag term, $nm_e^*\mathbf{u}^*\cdot(\langle\mathbf{v}\rangle-\mathbf{u})/\tau$, which appears usually in $\alpha(T)$ is neglected since its contribution for the longitudinal case is of order $\omega/4\pi\sigma_0$ (Ref. 25) and is negligible. For transverse attenuation this term would have to be included as it usually leads to the residual low-temperature sound attenuation in superconductors. The derivation of Eq. (4) does not depend on the use of the Boltzmann equation or the relaxation-time approximation which are used in Ref. 11.

The two dynamical conductivities $\sigma(\mathbf{q},\omega)$ and $\sigma^I(\mathbf{q},\omega)$ are calculated in linear-response theory using a diagrammatic formalism. $\sigma(\mathbf{q},\omega)$ depends on the impurity-averaged density-density correlation function $\rho(\mathbf{q},\omega)$ which is defined as

$$\rho(\mathbf{q},\omega)=-i\int\frac{d^3p}{(2\pi)^3}\int_{-\infty}^{\infty}\frac{d\omega'}{2\pi}\left[f\left[\omega'+\frac{\omega}{2}\right]-f\left[\omega'-\frac{\omega}{2}\right]\right]\Pi^{(1)}\left[\mathbf{p}+\frac{\mathbf{q}}{2},\mathbf{p}-\frac{\mathbf{q}}{2};\omega'+\frac{\omega}{2}+i\delta,\omega'-\frac{\omega}{2}-i\delta\right], \quad (5)$$

where

$$\Pi^{(1)}\left[\mathbf{p}+\frac{\mathbf{q}}{2},\mathbf{p}-\frac{\mathbf{q}}{2};\omega'+\frac{\omega}{2}+i\delta,\omega'-\frac{\omega}{2}-i\delta\right]$$
$$=\left\langle G\left[\mathbf{p}+\frac{\mathbf{q}}{2},\omega'+\frac{\omega}{2}+i\delta\right]G\left[\mathbf{p}-\frac{\mathbf{q}}{2},\omega'-\frac{\omega}{2}-i\delta\right]-F\left[\mathbf{p}+\frac{\mathbf{q}}{2},\omega'+\frac{\omega}{2}+i\delta\right]F^{\dagger}\left[\mathbf{p}-\frac{\mathbf{q}}{2},\omega'-\frac{\omega}{2}-i\delta\right]\right\rangle, \quad (6)$$

where[26]

$$G(\mathbf{p},\omega)=\frac{\tilde{\omega}(\omega)+\xi_p}{\tilde{\omega}^2(\omega)-\xi_p^2-|\Delta_{\mathbf{p}}|^2} \quad (7)$$

and[26]

$$F(\mathbf{p},\omega)=\frac{-\Delta_{\mathbf{p}}}{\tilde{\omega}^2(\omega)-\xi_p^2-|\Delta_{\mathbf{p}}|^2} \quad (8)$$

and $f(\omega)$ is $1/(e^{\beta\omega}+1)$. $\tilde{\omega}(\omega)$ and $\Delta_{\mathbf{p}}$ will be discussed presently.

The second conductivity, which arises in response to H_I, depends on the impurity average of the product of the density-density correlation function and the vertex $(1/m_e^*\omega)(\mathbf{q}\cdot\mathbf{p})(\mathbf{u}\cdot\mathbf{p})-(\mathbf{u}\cdot\mathbf{p})$, where terms of order q/k_F are ignored. This impurity-averaged product $\rho_I(\mathbf{q},\omega)$ is defined as

$$\rho_I(\mathbf{q},\omega)=i\int\frac{d^3p}{(2\pi)^3}\int_{-\infty}^{\infty}\frac{d\omega'}{2\pi}\left[f\left[\omega'+\frac{\omega}{2}\right]-f\left[\omega'-\frac{\omega}{2}\right]\right]\Pi_I^{(1)}\left[\mathbf{p}+\frac{\mathbf{q}}{2},\mathbf{p}-\frac{\mathbf{q}}{2};\omega'+\frac{\omega}{2}+i\delta,\omega'-\frac{\omega}{2}-i\delta\right], \quad (9)$$

where

$$\Pi_I^{(1)}\left[\mathbf{p}+\frac{\mathbf{q}}{2},\mathbf{p}-\frac{\mathbf{q}}{2};\omega'+\frac{\omega}{2}+i\delta,\omega'-\frac{\omega}{2}-i\delta\right]$$
$$=\left\langle\left[\frac{1}{m_e^*\omega}(\mathbf{q}\cdot\mathbf{p})(\mathbf{u}\cdot\mathbf{p})\right]\left[G\left[\mathbf{p}+\frac{\mathbf{q}}{2},\omega'+\frac{\omega}{2}+i\delta\right]G\left[\mathbf{p}-\frac{q}{2},\omega'-\frac{\omega}{2}-i\delta\right]\right.\right.$$
$$\left.\left.-F\left[\mathbf{p}+\frac{\mathbf{q}}{2},\omega'+\frac{\omega}{2}+i\delta\right]F^{\dagger}\left[\mathbf{p}-\frac{\mathbf{q}}{2},\omega'-\frac{\omega}{2}-i\delta\right]\right]\right\rangle$$
$$-\left\langle[(\mathbf{u}\cdot\mathbf{p})]\left[G\left[\mathbf{p}+\frac{\mathbf{q}}{2},\omega'+\frac{\omega}{2}+i\delta\right]G\left[\mathbf{p}-\frac{\mathbf{q}}{2},\omega'-\frac{\omega}{2}-i\delta\right]+F\left[\mathbf{p}+\frac{\mathbf{q}}{2},\omega'+\frac{\omega}{2}+i\delta\right]F^{\dagger}\left[\mathbf{p}-\frac{\mathbf{q}}{2},\omega'-\frac{\omega}{2}-i\delta\right]\right]\right\rangle. \quad (10)$$

In Eqs. (6) and (10), the complex conjugation operator on the last $F(\mathbf{p},\omega)$ Green's function only refers to the momentum dependence of the order parameter $\Delta_{\mathbf{p}}$. The conductivities $\sigma(\mathbf{q},\omega)$ and $\sigma^I(\mathbf{q},\omega)$ can then be written as

$$\sigma(\mathbf{q},\omega)=-\frac{i\omega}{q^2}\rho(\mathbf{q},\omega), \quad (11)$$

$$\sigma^I(\mathbf{q},\omega)=\frac{\omega}{q}\frac{\tau}{m_e^*u}\rho_I(\mathbf{q},\omega). \quad (12)$$

Impurity averaging results in a set of coupled linear equations for $\Pi^{(1)}$ and $\Pi_I^{(1)}$ which are written out fully in the Appendix. Apart from the vertex corrections introduced by impurity averaging, impurity effects are also included through $\tilde{\omega}(\omega)$ in $G(\mathbf{p},\omega)$ and $F(\mathbf{p},\omega)$. The temperature dependence of the order parameter depends on the level of impurity scattering also.

For the axial superconducting phase the renormalized frequencies $\tilde{\omega}(\omega)$ are given by[27]

$$\tilde{\omega}\left[\omega+\frac{\Omega}{2}+i\delta\right]=\omega+\frac{\Omega}{2}+i\delta-\frac{1}{2}\frac{\Gamma i\tilde{\omega}}{\Delta(T)}\ln\left[\frac{s\tilde{\omega}-\Delta(T)}{s\tilde{\omega}+\Delta(T)}\right], \quad (13)$$

where $s=\operatorname{sgn}\operatorname{Re}(\tilde{\omega}_{+i\delta})$ and $\Gamma=1/2\tau$. For the polar phase $\tilde{\omega}(\omega)$ is calculated from

$$\tilde{\omega}\left[\omega+\frac{\Omega}{2}+i\delta\right]=\omega+\frac{\Omega}{2}+i\delta+\frac{\Gamma\tilde{\omega}}{\Delta(T)}\ln\left[\frac{\Delta(T)-i[\tilde{\omega}^2-\Delta^2(T)]^{1/2}}{s'(-i)\tilde{\omega}}\right], \tag{14}$$

where $s'=\text{sgn Im}(\tilde{\omega}_{+i\delta})$.

The temperature-dependent order parameters for both phases, $\Delta(T)$, are obtained by solving the following coupled equations. For the axial phase[27]

$$1=\pi N_0\bar{V}T\tfrac{3}{2}\sum_n\frac{1}{2\Delta(T)}\left[\frac{|\tilde{\omega}_n|}{\Delta(T)}-\left[1-\frac{\tilde{\omega}_n^2}{\Delta^2(T)}\right]\frac{i}{2}\ln\left[\frac{i|\tilde{\omega}_n|-\Delta(T)}{i|\tilde{\omega}_n|+\Delta(T)}\right]\right], \tag{15}$$

where $N_0\bar{V}$ is the superconducting coupling constant and $\tilde{\omega}_n$ is the impurity renormalized Matsubara frequency given by

$$\tilde{\omega}_n(\omega_n)=\omega_n-i\Gamma\frac{\tilde{\omega}_n}{2\Delta(T)}\ln\left[\frac{i|\tilde{\omega}_n|-\Delta(T)}{i|\tilde{\omega}_n|+\Delta(T)}\right], \tag{16}$$

where $\omega_n=(2n+1)\pi T$.

For the polar phase, $\Delta(T)$ is obtained from [27]

$$1=\pi N_0\bar{V}T\tfrac{3}{2}\sum_n\frac{1}{\Delta(T)}\left\{\left[1+\left[\frac{\tilde{\omega}_n}{\Delta(T)}\right]^2\right]^{1/2}-\left[\frac{\tilde{\omega}_n}{\Delta(T)}\right]^2\ln\left[\frac{\Delta(T)+[\Delta^2(T)+\tilde{\omega}_n^2]^{1/2}}{|\tilde{\omega}_n|}\right]\right\}, \tag{17}$$

where

$$\tilde{\omega}_n(\omega_n)=\omega_n+\Gamma\frac{\tilde{\omega}_n}{\Delta(T)}\ln\left[\frac{\Delta(T)+[\Delta^2(T)+\tilde{\omega}_n^2]^{1/2}}{|\tilde{\omega}_n|}\right]. \tag{18}$$

Similar equations are defined for $\tilde{\omega}[\omega-(\Omega/2)-i\delta]$. In the numerical computation it is always assured[22] that $\tilde{\omega}(\omega+i\delta)=\tilde{\omega}^*(\omega-i\delta)$ and that

$$[\tilde{\omega}^2(\omega+i\delta)-\Delta^2(T)]^{1/2}=-\{[\tilde{\omega}^2(\omega-i\delta)-\Delta^2(T)]^{1/2}\}^*.$$

The equations for $\tilde{\omega}(\omega)$ are solved iteratively.

The superconducting density of states $N_s(\omega)$ can be obtained directly for both the axial and polar phases by

$$N_s(\omega)=N_0\frac{1}{\Gamma}\text{Im}(\tilde{\omega}_{+i\delta}). \tag{19}$$

Numerical results for $N_s(\omega)$ for both of these phases have been presented before.[27] A small degree of impurity scattering produces a rounding off of the peak in $N_s(\omega)$ near $\Delta(T)$. As the level of impurity scattering increases, $N_s(\omega)$ fills in at low frequencies. For a sufficiently high level of scattering a pronounced nonzero density of states exists at zero frequency. For the polar case, $N_s(0)$ is nonzero for any value of Γ while for the axial state $N_S(0)\neq 0.0$ only for $\Gamma\geq(2/\pi)\Delta$. However for any $\Gamma\geq 0.3\Delta$, a large filling in of $N_S(\omega)$ at low frequencies occurs in the case of both phases.

It is worth noting that the effect of pairbreaking on $N_S(\omega)$ due to impurity scattering will increase strongly near T_c, even when the level of impurity scattering is weak, for example $\Gamma\leq 0.1\Delta(0)$. This is due to the fact that near T_c $\Delta(T)$ becomes very small and so the effective pairbreaking parameter $1/2\tau\Delta(T)$ in the calculation on $N_S(\omega)$ increases dramatically.

NUMERICAL RESULTS AND DISCUSSION

In order to generate $\alpha(T)$ curves, the values of the parameters v_s/v_F and T_c/T_F must be specified first. This is similar to Ref. 17. For heavy fermion materials, v_s/v_F and T_c/T_F would be expected to be of order 1.0 and 0.1, respectively. For most of the ultrasonic attenuation curves presented here v_s/v_F was chosen to be $\frac{2}{3}$ and T_c/T_F to be 0.04 for the polar and 0.05 for the axial phase. Other values have been investigated and are discussed.

Ultrasonic attenuation results for the polar case with $\Delta_p=\Delta(T)\hat{\mathbf{p}}_z$ and $\hat{\mathbf{q}}\|\hat{\mathbf{z}}$ are plotted in Figs. 1 to 5. The ql and $\omega\tau$ values are indicated on the figures and range from 0.045 to 15.0 and from 0.03 to 10.0, respectively.

Results for the axial phase with $\Delta_p=\Delta(T)(\mathbf{p}_x+i\mathbf{p}_y)$ and $\hat{\mathbf{q}}\|\hat{\mathbf{x}}$ are plotted in Figs. 6 to 8. The corresponding ql and $\omega\tau$ values range from 0.15 to 4.5 and 0.10 to 3.0, respectively. In all the figures, $\alpha(T)$ is plotted in units of $nm_e^*/\rho c_s\tau$ which is defined in Eq. (4).

The values of ql and v_s/v_F chosen in this calculation are in the same range as experimentally observed values for these quantities. For example, attenuation measurements[1] on UPt_3 at 500 MHz yield a sound wavelength of 10 μm. The mean free path is thought to be greater than 1000 Å in this case, thus giving a ql value of 0.06 or more. In UBe_{13}, attenuation measurements[2] have been carried out at 1.7 GHz, yielding a ql value of 0.2 or more.

Furthermore, recent de Haas–van Alphen measurements[28] on UPt_3 have indicated measurements of the cyclotron mass to be 25–90 times the bare electron mass. These measurements indicate 8 pockets of electrons and holes for UPt_3. Using 20 g cm^{-3} as an estimate for the density of UPt_3,[29] these observations yield k_F to be 0.4×10^8 cm^{-1} and $v_F=\hbar k_F/m_e^*$ to be between 0.18×10^7 cm sec^{-1} and 0.05×10^7 cm sec^{-1}. Taking v_s for UPt_3 to be 4×10^5 cm sec^{-1} (Ref. 18) yields values of v_s/v_F ranging

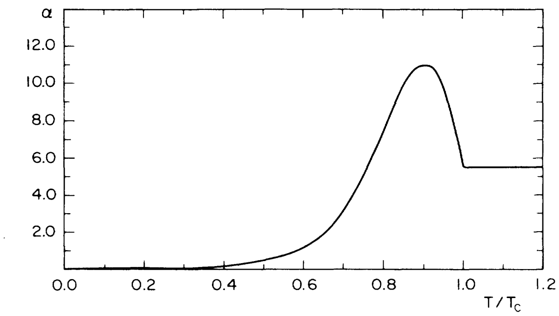

FIG. 1. $\alpha(T)$ for the polar state with $\hat{\mathbf{q}}\|\hat{\mathbf{z}}$, $ql=15.0$, $\omega\tau=10.0$, $E_F\tau=5\times10^4$, and $\Delta(0)\tau=5\times10^3$.

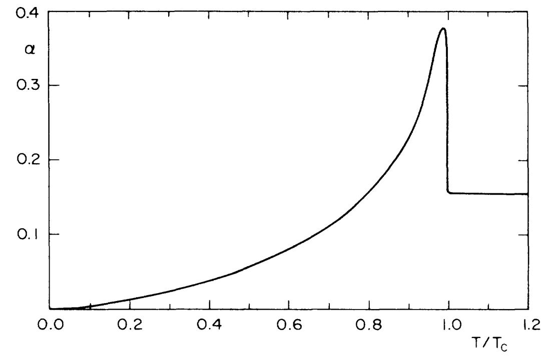

FIG. 3. $\alpha(T)$ for the polar state with $\hat{\mathbf{q}}\|\hat{\mathbf{z}}$, $ql=0.9$, $\omega\tau=0.6$, $E_F\tau=3000$, and $\Delta(0)\tau=300.0$.

ing from 0.22 to 0.78. Thus the value chosen for v_s/v_F ($\frac{2}{3}$) in this calculation is not unreasonable.

Clear exponents describing the low to intermediate temperature dependence of the $\alpha(T)$ curves in Figs. 1–8 can be obtained and are listed in Table I. On first examination some of the curves produced are very similar to the experimental results.[1–3] For example in the polar case the $\alpha(T)$ curve for $ql=0.9$ and $\omega\tau=0.6$ has a T^2 temperature dependence over most of its range and also has a peak which is similar in size and shape to that of Ref. 2. Furthermore, the $\alpha(T)$ curves can have a T^2 or a T^3 dependence depending on the level of disorder, in agreement with other experimental results on UPt_3. Most surprising of all, the peak observed in $\alpha(T)$ below T_c is reproduced in very good agreement with experiments.

Before discussing this peak, the question of which superconducting phase describes the experiments best should be addressed. The first observation is that both the axial and the polar phases do so equally well. The lack of a unique, disorder independent exponent characterizing the low-temperature behavior seems to rule the possibility of, for example, clearly identifying a T^2 dependence with the polar phase exclusively. Only a careful determination of the parameters E_F and τ, coupled with a series of measurements of $\alpha(T)$ on the same sample while increasing the level of disorder in it systematically, could hope to succeed in saying anything conclusive on this issue.

As can be seen from Figs. 1–8, the present calculation produces a peak in α just below T_c. For certain realistic values of ql, this peak looks very similar qualitatively to that observed in experiments.[2,3] A peak in $\alpha(T)$ is also observed in the theoretical work of Ref. 17, although, as the authors of that work point out, their calculation was not in a physically relevant limit.

Along with the results shown in Figs. 1 to 8, the peak was investigated with τ fixed and ω and q varying in the range $ql=0.03$ to 4.5 and $\omega\tau=0.02$ to 3.0. The peaks in $\alpha(T)$ that are generated do not seem to have the characteristics of the Landau-Khalatnikov mechanism of Ref. 18. For fixed τ and variable ω, the difference between the peak height and α_n, $\Delta\alpha$, is proportional to $\omega^{1.5}$ rather than ω and this exponent varies with changes in v_s/v_F and T_c/T_F. Furthermore, the Landau-Khalatnikov mechanism would predict a constant value for $\Delta\alpha$ when ω is fixed and τ is varied. In this calculation however, when the $\alpha(T)$ curves are normalized by the same constant, $\Delta\alpha$ still changes. Finally while the peak position shifts away from T_c as τ is increased, its position is still different to the Landau-Khalatnikov prediction of $\omega\tau\approx(1-T_p/T_c)^2$. One can conclude from this numerical investigation that

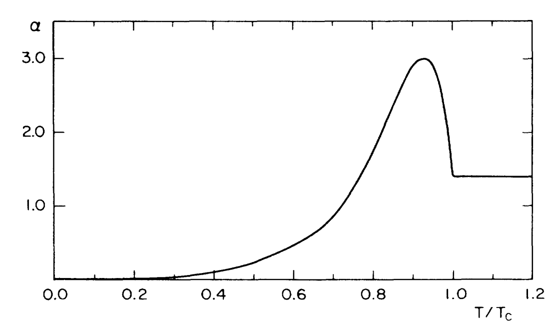

FIG. 2. $\alpha(T)$ for the polar state with $\hat{\mathbf{q}}\|\hat{\mathbf{z}}$, $ql=4.5$, $\omega\tau=3.0$, $E_F\tau=1.5\times10^4$, and $\Delta(0)\tau=1.5\times10^3$.

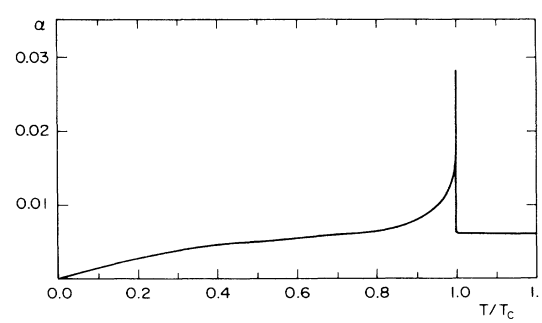

FIG. 4. $\alpha(T)$ for the polar state with $\hat{\mathbf{q}}\|\hat{\mathbf{z}}$, $ql=0.15$, $\omega\tau=0.1$, $E_F\tau=500$, and $\Delta(0)\tau=50.0$.

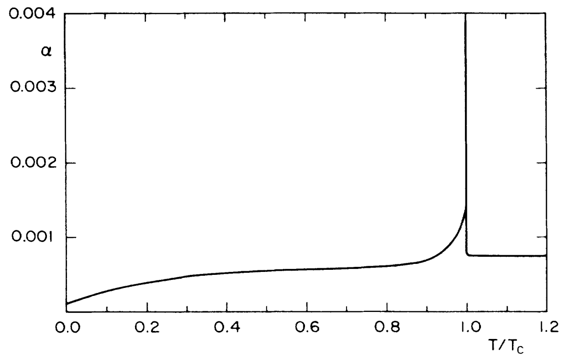

FIG. 5. $\alpha(T)$ for the polar state with $\hat{\mathbf{q}}\|\hat{\mathbf{z}}$, $ql=0.045$, $\omega\tau=0.03$, $E_F\tau=150$, and $\Delta(0)\tau=15.0$.

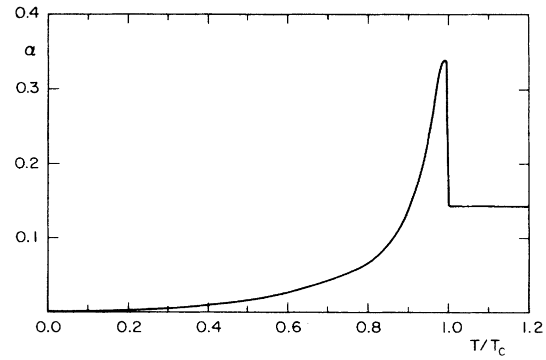

FIG. 7. $\alpha(T)$ for the axial state with $\hat{\mathbf{q}}\|\hat{\mathbf{x}}$, $ql=0.9$, $\omega\tau=0.6$, $E_F\tau=3000$, and $\Delta(0)\tau=300.0$.

processes other than this mechanism are contributing to the peak in $\alpha(T)$. Thus the Landau-Khalatnikov mechanism does not seem to be the complete explanation for the whole peak.

An interesting point highlighted by Ref. 18 is the importance of the pairbreaking time τ due to impurity scattering. If τ plays a major role in producing the peak, as suggested by Ref. 18, then such a peak should also be observable in magnetically impure superconductors where the pairbreaking time due to magnetic scattering would play the role of τ. Such an observation could test the importance of the Landau-Khalatnikov mechanism in producing a peak in $\alpha(T)$.

However the existence of the peak could be due to a combination of factors. Close to T_c the effective pairbreaking parameter that enters the calculation of $N_s(\omega)$, that is $\Gamma=1/2\Delta(T)\tau$, will increase dramatically. The resulting filling in of the low frequency $N_s(\omega)$ could then lead to a large contribution from Cooper pairbreaking by the sound wave, that is excitation of quasiparticles across the "gap," thus producing a peak near T_c.

Furthermore a role may be being played by the sound attenuation coherence factor, $(1-|\Delta_p|^2/E_p^2)$. For those regions of the Fermi surface where Δ_p is small, this factor is larger than the conventional BCS value. Near T_c, where the number of thermally excited quasiparticles is appreciable, the peak in $N_s(\omega)$ may be rendered visible as a result. Normally in the BCS case the smallness of the coherence factor cancels out the peak in $N_s(\omega)$ and no increase is seen in $\alpha(T)$ below T_c.

One other test of the predictions of the present theory would be to examine experimentally the behavior of the peak as τ is decreased. This calculation predicts that the peak in $\alpha(T)$ should sharpen up considerably and move closer to T_c.

The effect of strong pairbreaking due to impurity scattering on $\alpha(T)$ in the polar phase can be seen in Fig. 9. Here $\Delta(0)\tau=1.7$, $ql=0.15$, and $\omega\tau=0.1$. The peak height has diminished and a large nonzero sound attenuation is visible at zero temperature. This effect is a reflection of the filling in of $N_s(\omega)$ at low frequencies due to the smallness of τ.

Allowing v_s/v_F and T_c/T_F to both approach zero has a considerable effect on the shape of the $\alpha(T)$ curve. This is shown for the polar case in Fig. 10 for $\Delta(0)\tau=1.5$ and the ql and $\omega\tau$ values indicated on the figure. The values of v_s/v_F and T_c/T_F here are 2×10^{-2} and 1.2×10^{-3}, respectively. Choosing these parameter values necessarily forces one into the strong pair-breaking limit. This is due to the fact that for reasonable mean free paths ($l=1000$ Å), k_Fl is of the order of 1000 and thus $E_F\tau$ of the order of 500. Thus for T_c/T_F of the order of 10^{-3} this requires $\Delta(0)\tau$ to be of the order of 1.0. As can be seen in Fig. 10 the curves generated for these values look totally unlike

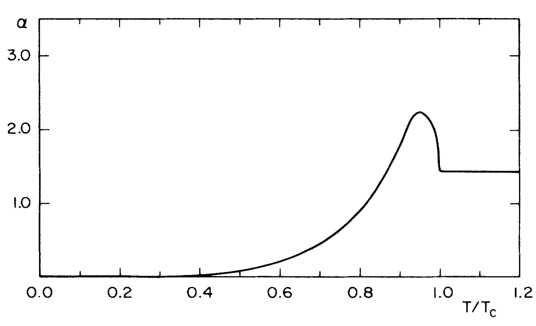

FIG. 6. $\alpha(T)$ for the axial state with $\hat{\mathbf{q}}\|\hat{\mathbf{x}}$, $ql=4.5$, $\omega\tau=3.0$, $E_F\tau=1.5\times10^4$, and $\Delta(0)\tau=1500.0$.

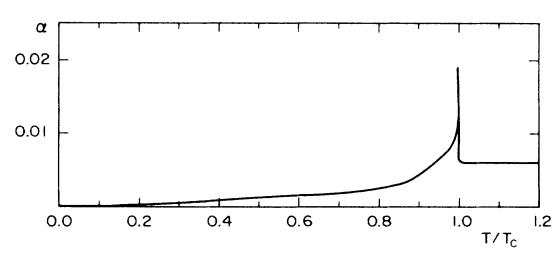

FIG. 8. $\alpha(T)$ for the axial state with $\hat{\mathbf{q}}\|\hat{\mathbf{x}}$, $ql=0.15$, $\omega\tau=0.1$, $E_F\tau=500.0$, and $\Delta(0)\tau=50.0$.

TABLE I. Exponents characterizing the longitudinal ultrasonic attenuation curves in Figs. 1–8, along with the corresponding values of ql, $\omega\tau$, $\Delta(0)\tau$, and T/T_c.

ql	$\omega\tau$	Temperature range (T/T_c)	$\Delta(0)\tau$	$\alpha(T)$
		Polar		
0.045	0.03	0.35–0.75	15.0	$0.00045+0.00018(T/T_c)$
0.15	0.1	0.30–0.8	50.0	$0.0025+0.0049(T/T_c)$
0.9	0.6	0.10–0.8	300.0	$0.27(T/T_c)^2$
4.5	3.0	0.30–0.85	1500.0	$3.94(T/T_c)^{3.75}$
15.0	10.0	0.20–0.5	5000.0	$5.75(T/T_c)^{3.7}$
		Axial		
0.15	0.1	0.30–0.7	50.0	$0.0038(T/T_c)^{1.5}$
0.9	0.6	0.30–0.7	300.0	$0.1290(T/T_c)^{3.0}$
4.5	3.0	0.10–0.7	1500.0	$2.1860(T/T_c)^{4.5}$

the experimental observations. The choice of v_s/v_F and T_c/T_F used in Figs. 1–8 is necessary in order to obtain good agreement with experiments. This choice fits in with the simple interpretation that the quasiparticles taking place in the sound attenuation process are heavy fermions.

Ultrasonic attenuation curves for the polar state were examined choosing v_s/v_F to be small while keeping T_c/T_F to be of the order of 0.1. Results qualitatively similar to those of Ref. 17 were obtained with $\alpha(T)$ increasing to large nonzero value at $T=0.0$ if $\hat{\mathbf{q}}$ was along $\hat{\mathbf{z}}$. With $\hat{\mathbf{q}}$ displaced slightly away from $\hat{\mathbf{z}}$, $\alpha(T)$ has a broad maximum and drops to zero at zero temperature.

Finally, the effect on α of $\hat{\mathbf{q}}$ vectors along arbitrary directions on the Fermi surface has not been examined completely yet. However preliminary results for the polar phase with $\hat{\mathbf{q}}\|\hat{\mathbf{x}}$ and $\Delta_p=\Delta(T)\mathbf{p}_z$ indicate no major qualitative change in $\alpha(T)$. The curve obtained is quantitatively similar to that for $\hat{\mathbf{q}}\|\hat{\mathbf{z}}$ and there is still a peak below T_c. Further investigations of arbitrary directions for $\hat{\mathbf{q}}$ will be carried out.

CONCLUSIONS

The present calculation of longitudinal ultrasonic attenuation for axial and polar anisotropic superconducting phases has yielded theoretical curves that are in reasonable agreement with experiments. This is the case for physically realistic values of ql and $\omega\tau$. Furthermore, this is true not only from the point of view of the exponents describing the low to intermediate temperature dependence but also concerning the peak near T_c. In the absence of experiments carefully determining the parameters in the calculation, it is difficult to distinguish at the moment which of the two types of anisotropic superconducting phases, polar or axial, best fits the data. The different temperature exponents seen for different samples of the same superconductor, that is UPt_3, are explicable as an impurity effect. Furthermore, it seems reasonable that the peak in $\alpha(T)$ is due to the combination of increased Cooper pairbreaking and coherence factor effects discussed earlier in the presentation of numerical results. Finally the need to choose v_s/v_F and T_c/T_F to be of the order of 1.0 and 0.1, respectively, rather than the normal values, in order to achieve agreement with experiments, lends support to the idea that the quasiparticles taking part in the attenuation process are heavy fermions with v_s comparable to v_F. Further studies are to examine the effects on $\alpha(T)$ of choosing directions for $\hat{\mathbf{q}}$ other than those considered here.

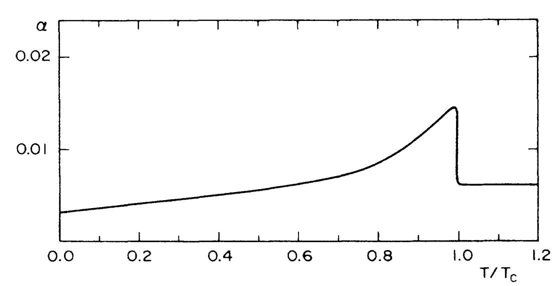

FIG. 9. $\alpha(T)$ for the polar state with $\hat{\mathbf{q}}\|\hat{\mathbf{z}}$, $ql=0.15$, $\omega\tau=0.1$, $E_F\tau=50.0$, and $\Delta(0)\tau=1.7$.

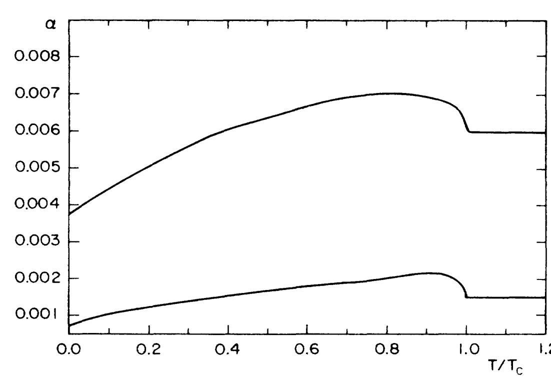

FIG. 10. $\alpha(T)$ for the polar state with $\hat{\mathbf{q}}\|\hat{\mathbf{z}}$, $ql=0.15$, $\omega\tau=0.003$, $E_F\tau=500.0$, and $\Delta(0)\tau=1.5$ (upper curve). $\alpha(T)$ for the polar state with $\hat{\mathbf{q}}\|\hat{\mathbf{z}}$, $ql=0.07$, $\omega\tau=0.0015$, $E_F\tau=500.0$, and $\Delta(0)\tau=1.5$ (lower curve).

ACKNOWLEDGMENTS

I wish to acknowledge T. M. Rice for informative discussions and for reading the initial draft of the manuscript. I would also like to thank R. Joynt and K. Ueda for discussions and correspondence. The support of Schweizer Nationalfonds is gratefully acknowledged.

APPENDIX

The coupled linear equations for the vertex corrections arising from impurity averaging in Eqs. (6) and (10) are written as follows. Firstly typical integrals of products of Green's functions occurring in these equations are defined in the following notation:

$$G_+(\omega_+)G_-(\omega_-)=n_i u^2\int\frac{d^3p}{(2\pi)^3}G\left[\mathbf{p}+\frac{\mathbf{q}}{2};\omega+\frac{\Omega}{2}+i\delta\right]\times G\left[\mathbf{p}-\frac{\mathbf{q}}{2};\omega-\frac{\Omega}{2}-i\delta\right], \tag{A1}$$

where n_i is the concentration of impurities, u is the scattering potential, and Ω is the sound frequency. G can be either $G(\mathbf{p},\omega)$ or $F(\mathbf{p},\omega)$. So, for example,

$$G_-(\omega_-)F_+(\omega_+)=n_i u^2\int\frac{d^3p}{(2\pi)^3}G\left[\mathbf{p}-\frac{\mathbf{q}}{2};\omega-\frac{\Omega}{2}-i\delta\right]\times F\left[\mathbf{p}+\frac{\mathbf{q}}{2};\omega+\frac{\Omega}{2}+i\delta\right]. \tag{A2}$$

Replacing $\int d^3p/(2\pi)^3$ with

$$N_0\int_{-\infty}^{\infty}d\xi_p\int\frac{\sin\theta\, d\theta\, d\Phi}{4\pi},$$

where N_0 is the density of states at the Fermi level, the integral over ξ_p can be performed in the usual way by contour integration.[26] The remaining angular integrations over θ and ϕ can be performed numerically. Furthermore,

$$\int\frac{d^3p}{(2\pi)^3}\Pi^{(1)}\left[\mathbf{p}+\frac{\mathbf{q}}{2},\mathbf{p}-\frac{\mathbf{q}}{2};\omega+\frac{\Omega}{2}+i\delta,\omega-\frac{\Omega}{2}-i\delta\right]$$

is written as $\Pi^{(1)}$ for brevity. Using this notation,

$$\begin{aligned}\Pi^{(1)}=&\,G_+(\omega_+)G_-(\omega_-)-F_+(\omega_+)F_-^{\dagger}(\omega_-)\\&+\Pi^{(1)}G_+(\omega_+)G_-(\omega_-)+\Pi^{(4)}G_+(\omega_+)F_-^{\dagger}(\omega_-)\\&-\Pi^{(2)}G_-(\omega_-)F_+(\omega_+)-\Pi^{(3)}F_+(\omega_+)F_-^{\dagger}(\omega_-)\,,\end{aligned} \tag{A3}$$

$$\begin{aligned}\Pi^{(2)}=&\,G_-(\omega_-)F_+^{\dagger}(\omega_+)+G_+(-\omega_+)F_-^{\dagger}(\omega_-)\\&+\Pi^{(2)}G_-(\omega_-)G_+(-\omega_+)+\Pi^{(1)}G_-(\omega_-)F_+^{\dagger}(\omega_+)\\&+\Pi^{(3)}G_+(-\omega_+)F_-^{\dagger}(\omega_-)+\Pi^{(4)}F_-^{\dagger}(\omega_-)F_+^{\dagger}(\omega_+)\,,\end{aligned} \tag{A4}$$

$$\begin{aligned}\Pi^{(3)}=&\,G_-(-\omega_-)G_+(-\omega_+)-F_+^{\dagger}(\omega_+)F_-(\omega_-)\\&+\Pi^{(3)}G_+(-\omega_+)G_-(-\omega_-)\\&-\Pi^{(2)}G_+(-\omega_+)F_-(\omega_-)\\&+\Pi^{(4)}G_-(-\omega_-)F_+^{\dagger}(\omega_+)-\Pi^{(1)}F_-(\omega_-)F_+^{\dagger}(\omega_+)\,,\end{aligned} \tag{A5}$$

$$\begin{aligned}\Pi^{(4)}=&\,-G_-(-\omega_-)F_+(\omega_+)-G_+(\omega_+)F_-(\omega_-)\\&+\Pi^{(4)}G_+(\omega_+)G_-(-\omega_-)-\Pi^{(3)}G_-(-\omega_-)F_+(\omega_+)\\&+\Pi^{(2)}F_-(\omega_-)F_+(\omega_+)-\Pi^{(1)}G_+(\omega_+)F_-(\omega_-)\,.\end{aligned} \tag{A6}$$

The complex conjugation on the $F(\mathbf{p},\omega)$ Green's function only means that the momentum dependence of the order parameter in the numerator of $F(\mathbf{p},\omega)$ should be complex conjugated and not the whole Green's function.

The equations for $\Pi_I^{(1)}$ to $\Pi_I^{(4)}$ which result from the first term in H_I, i.e., $(1/m_e^*\Omega)(\mathbf{q}\cdot\mathbf{p})(\mathbf{u}\cdot\mathbf{p})$ are identical to equations (A3) to (A6) except that the first two Green's function products on the right-hand side of these equations are multiplied by the vertex $(1/m_e^*\Omega)(\mathbf{q}\cdot\mathbf{p})(\mathbf{u}\cdot\mathbf{p})$ before the integral over $\mathbf{p}$ is performed as described in (A1). In the case of the second contribution from H_I, i.e., $-(\mathbf{u}\cdot\mathbf{p})$ $\Pi_I^{(1)}-\Pi_I^{(4)}$ are again given by equations very similar to Eqs. (A3) and (A6), except that the first two Green's function products on the right-hand side of these equations are, before the integral over $\mathbf{p}$ is performed, replaced by

$$G_+(\omega_+)G_-(\omega_-)+F_+(\omega_+)F_-^{\dagger}(\omega_-)\,,$$

$$G_-(\omega_-)F_+^{\dagger}(\omega_+)-G_+(-\omega_+)F_-^{\dagger}(\omega_-)\,,$$

$$-G_-(-\omega_-)G_+(-\omega_+)-F_+^{\dagger}(\omega_+)F_-(\omega_-)\,,$$

$$G_-(-\omega_-)F_+(\omega_+)-G_+(\omega_+)F_-(\omega_-)\,,$$

respectively, each of these terms being multiplied by the vertex $-(\mathbf{u}\cdot\mathbf{p})$. These coupled equations for $\Pi^{(1)}-\Pi^{(4)}$ and $\Pi_I^{(1)}-\Pi_I^{(4)}$ are inverted using the International Mathematics and Statistical Library (IMSL) routine LEQT1C.

*Present address: Department of Physics, Ohio State University, Columbus, OH 43210-1106.

[1]D. J. Bishop, C. M. Varma, B. Batlogg, E. Bucher, Z. Fisk, and J. L. Smith, Phys. Rev. Lett. **53**, 1009 (1984).

[2]B. Golding, D. J. Bishop, B. Batlogg, W. H. Haemmerle, Z. Fisk, J. L. Smith, and H. R. Ott, Phys. Rev. Lett. **55**, 2479 (1985).

[3]V. Muller, D. Maurer, E. W. Scheidt, C. Roth, K. Luders, E.

Bucher, and H. Bommel, Solid State Commun. **57**, 319 (1986).
[4]B. Batlogg, D. Bishop, B. Golding, C. M. Varma, Z. Fisk, J. L. Smith, and H. R. Ott, Phys. Rev. Lett. **55**, 1319 (1985).
[5]P. W. Anderson, Phys. Rev. B **30**, 4000 (1984).
[6]G. E. Volovik and L. P. Gorkov, Pis'ma Zh. Eksp. Teor. Fiz. **39**, 550 (1984) [JETP Lett. **39**, 674 (1984)].
[7]E. I. Blount, Phys. Rev. B **32**, 2395 (1985).
[8]K. Ueda and T. M. Rice, Phys. Rev. B **31**, 7114 (1985).
[9]K. Ueda and T. M. Rice, in *Advances in Solid State Physics*, edited by P. Grosse (Vieweg, Braunschweig, 1985), Vol. XXV, p. 209.
[10]G. E. Volovik and L. P. Gorkov, Zh. Eksp. Teor. Fiz. **88**, 1412 (1985) [Soviet Physics—JETP **61**, 843 (1985)].
[11]J. P. Rodriguez, Phys. Rev. Lett. **55**, 250 (1984).
[12]L. Coffey, T. M. Rice, and K. Ueda, J. Phys. C **18**, L813 (1985); J. Phys. C **19**, 1079(C) (1986).
[13]C. J. Pethick and D. Pines, Phys. Rev. Lett. **57**, 118 (1986).
[14]S. Schmitt-Rink, K. Miyake, and C. M. Varma, Phys. Rev. Lett. **57**, 2575 (1986).
[15]P. Hirschfeld, D. Vollhardt, and P. Wolfle, Solid State Commun. **59**, 111 (1986).
[16]K. Scharnberg, D. Walker, H. Monien, L. Tewordt, and R. A. Klemm, Solid State Commun. **60**, 535 (1986).
[17]S. N. Coppersmith and R. A. Klemm, Phys. Rev. Lett. **56**, 1870 (1986).
[18]K. Miyake and C. M. Varma, Phys. Rev. Lett. **57**, 1627 (1986).
[19]R. Takke, M. Niksch, W. Assums, B. Lüthi, R. Pott, R. Schefzyk, and K. D. Wohlleben, Z. Phys. B **44**, 33 (1981).
[20]K. Becker and P. Fulde, Z. Phys. B **65**, 313 (1987).
[21]T. Tsuneto, Phys. Rev. **121**, 402 (1961).
[22]L. P. Kadanoff and I. I. Falko, Phys. Rev. **136**, A1170 (1964).
[23]E. I. Blount, Phys. Rev. **114**, 418 (1959).
[24]See, for example, C. Kittel, *Quantum Theory of Solids* (Wiley, New York, 1963), p. 330.
[25]M. H. Cohen, M. J. Harrison, and W. A. Harrison, Phys. Rev. **117**, 937 (1960).
[26]See, for example, A. A. Abrikosov, L. P. Gorkov, and I. E. Dzyaloshinski, *Methods of Quantum Field Theory in Statistical Physics* (Dover, New York, 1963).
[27]K. Ueda and T. M. Rice, Proceedings of the 8th Taniguchi Symposium on the Theory of Valence Fluctuating State, 1985 (in press).
[28]L. Taillefer, R. Newbury, G. G. Lonzarich, Z. Fisk, and J. L. Smith, Proceedings of ICAREA, Grenoble, 1986 (in press).
[29]J. W. Chen, S. E. Lambert, M. B. Maple, Z. Fisk, J. L. Smith, G. R. Stewart, and J. O. Willis, Phys. Rev. B **30**, 1583 (1984).